J. Phys. G: Nucl. Part. Phys. 21 (1995) 1101–1119. Printed in the UK

Muons ($\geqslant$ 1 GeV) in large extensive air showers of energies between $10^{16.5}$ eV and $10^{19.5}$ eV observed at Akeno

N Hayashida[(1)], K Honda[(2)], M Honda[(1)], S Imaizumi[(3)]†, N Inoue[(3)], K Kadota[(4)], F Kakimoto[(4)], K Kamata[(5)], S Kawaguchi[(6)], N Kawasumi[(2)], Y Matsubara[(7)], K Murakami[(8)], M Nagano[(1)], H Ohoka[(1)], M Takeda[(4)], M Teshima[(1)], I Tsushima[(2)], S Yoshida[(9)] and H Yoshii[(10)]

[(1)] Institute for Cosmic Ray Research, University of Tokyo, Tokyo 188, Japan
[(2)] Faculty of Education, Yamanashi University, Kofu 400, Japan
[(3)] Department of Physics, Saitama University, Urawa 338, Japan
[(4)] Department of Physics, Tokyo Institute of Technology, Tokyo 152, Japan
[(5)] Nishina Memorial Foundation, Tokyo 188, Japan
[(6)] Faculty of General Education, Hirosaki University, Hirosaki 036, Japan
[(7)] Solar-Terrestrial Environment Laboratory, Nagoya University, Nagoya 464-01, Japan
[(8)] Nagoya University of Foreign Studies, Nissin, Aichi 470-01, Japan
[(9)] High Energy Astrophysics Institute, Department of Physics, University of Utah, Salt Lake City, UT 84112, USA
[(10)] Faculty of General Education, Ehime University, Matsuyama 790, Japan

Received 27 April 1995

Abstract. The properties of muons ($\geqslant$ 1 GeV) in giant air showers between $10^{16.5}$ eV and $10^{19.5}$ eV are measured by the Akeno 1 km^2, 20 km^2 and 100 km^2 air shower arrays. The lateral distribution of muons is well fitted by the formula given by Greisen with parameters $\beta = 2.52\pm0.02$ and $\log(R_0) = (0.58\pm0.04)(\sec\theta-1)+(2.39\pm0.05)$ between $10^{16.5}$ eV and $10^{19.0}$ eV within 800 m of the air shower axis, where θ is the zenith angle of the shower arrival direction. The relation between the total number of muons (N_μ) and the total number of electrons (N_e) derived using these parameters is expressed on average as $N_\mu = (2.6\pm1.3)\times10^{5.0+a}(N_e/10^7)^b$, where $a = (1.07\pm0.13)(\sec\theta-1)$ and $b = (0.77\pm0.02)-(0.17\pm0.02)(\sec\theta-1)$. The lateral distribution of muons becomes steeper than expected from extrapolation of the above formula for core distances > 800 m and is expressed as $\rho_\mu = N_\mu(C'_\mu/R_0^2)r^{-0.75}(1+r)^{-\beta}[1+(R/800\text{ m})^3]^{-\delta}$ ($r = R/R_0$, where R is a core distance). No deviation from this formula has been observed for $\sec\theta < 2.0$ up to $10^{19.0}$ eV. The relation between the muon density ($\rho_\mu(600)$) and the charged-particle density on the ground at 600 m from the core ($S(600)$) is studied between $10^{16.5}$ eV and $10^{19.0}$ eV. A systematic change in the chemical composition of cosmic rays from a predominantly heavy to a predominantly light composition above $10^{17.5}$ eV claimed by the Fly's Eye group has not been detected beyond the present experimental uncertainties. The present experiment suggests a much smaller rate of change of composition between $10^{17.5}$ eV and $10^{18.5}$ eV than that from the Fly's Eye experiment.

1. Introduction

Muons of energies around 1 GeV are one of the important observables in extensive air showers (EAS) produced by very energetic cosmic rays. In order to determine the energy and the arrival direction of cosmic rays of the highest energies, the Sydney group (Winn *et*

† Now at Casio Co Ltd, Hamura 205, Japan.

0954-3899/95/081101+19$19.50

al 1986) has measured muons of threshold energy 0.75 GeV in large EAS. This is because the total number of muons (N_μ) attenuates more slowly with atmospheric depth than that of electrons (N_e) after their maximum development and hence N_μ may be a good energy estimator of primary cosmic rays. The main disadvantage of using muons as an energy estimator is that N_μ is much smaller than N_e, and hence a larger detector is required for measuring muons. Another disadvantage is that N_μ is quite sensitive to the model of hadronic interactions and the chemical composition of primary cosmic rays. The latter characteristics are, however, considered to be an advantage for investigation of the models of hadronic interactions beyond accelerator energies and the chemical composition in the high-energy region where direct measurements of charges of primary particles are not attainable, provided the primary energy is estimated by other components.

Recently, the Yakutsk group claimed that the slope of the lateral distribution of muons above 5×10^{18} eV changes significantly from that at lower energies and that the attenuation length of N_μ becomes very large, while N_e attenuates quite quickly in this energy region. For example, their largest energy event, which has an energy of about 1.2×10^{20} eV and a zenith angle of 60°, consists almost entirely of muons of energies above 2 GeV at ground level. The group considers that this may be connected with some new process of EAS development (Glushkov *et al* 1994) in the energy region above 5×10^{18} eV. In order to determine the energy and zenith-angle dependence of the lateral distribution, careful study is required so as not to bias the distance range concerned, which depends heavily on the primary energy.

The Fly's Eye group reported the energy dependence of the depth at shower maximum (X_{max}) and showed that a change in the elongation rate ($\delta X_{max}/\delta \ln E$) is observed around 3×10^{17} eV (Bird *et al* 1993). They claim that this change is evidence for a change from a predominantly heavy to a predominantly light composition around that energy. Since N_μ from heavy primaries is larger than that from light ones for equal primary energies, the ratio of the muon component to the electron component may become smaller than the extrapolated value from the lower energy region in this energy range, if the Utah group's finding is due to a change in the primary composition.

The observation of extremely high energy cosmic rays well beyond the proposed 2.7 K cut-off of the primary spectrum (Bird *et al* 1994, Hayashida *et al* 1994) has stimulated plans for the next generation experiment. The construction of a giant air shower array of area 5000 km^2 is being planned (Cronin 1992). In this array, a sandwich detector, consisting of a sandwich of a thin top detector, a lead sheet (~2 r.l.) and a thin bottom detector, is proposed to separate the muonic component from the electromagnetic component far from the core. The design of this kind of detector requires the determination of the lateral distributions of electrons and muons at core distances exceeding 1000 m.

The characteristics of the muon component are described here using data obtained by three different experiments at Akeno. In section 2, details of the experiments at the Akeno Air Shower Observatory are described. In section 3, the lateral distribution of muon densities (ρ_μ) is examined between $10^{16.5}$ eV and $10^{19.0}$ eV for both vertical and inclined showers with core distances $\leqslant$ 800 m. The lateral distribution of ρ_μ for core distances exceeding 800 m is derived in comparison with that for core distances $\leqslant$ 800 m. The relationships between N_μ and N_e, and between $\rho_\mu(600)$ and $S(600)$ are derived using the lateral distribution thus obtained, where $\rho_\mu(600)$ and $S(600)$ are the densities of muon and charged particles on the surface at 600 m from the core, respectively. In section 4, the present results are compared with those given by other experiments and with simulated results. The relation between $\rho_\mu(600)$ and $S(600)$ is discussed at the end of the section, in the light of primary cosmic-ray composition.

2. Experiment

2.1. General

The experiment has been performed at Akeno at 900 m above sea level. The whole array consists of several arrays of different detector separations in order to cover the wide primary energy range. The arrays related to the present experiment are shown in figure 1.

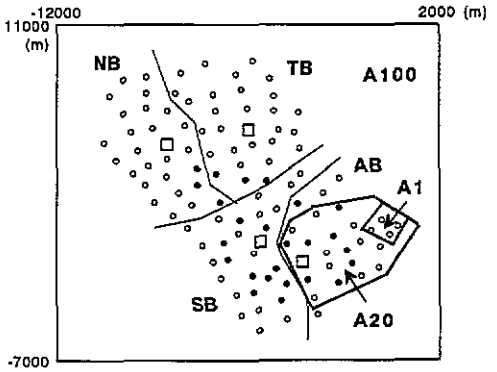

Figure 1. A schematic diagram of the Akeno giant air shower array (AGASA, A100). The relationship between AGASA (A100), the 1 km^2 array (A1) and the 20 km^2 array (A20) is shown.

The 1 km^2 air shower array (hereafter denoted by A1, Hara *et al* 1979) consists of 156 scintillation counters of area 1 m^2 each, deployed on the surface over an area of approximately 1 km^2 with eight muon detectors of area 25 m^2 each. The surface detectors have been operated since 1979 and the muon detectors since October 1981. The triggering requirement for the present analysis is a coincidence of at least seven out of 37 surface detectors mutually separated by 120 m. This array is designed for studies of EAS between $10^{16.5}$ eV and $\sim 10^{18.5}$ eV. The absorber of the electromagnetic component over the muon detectors is concrete shielding of 2 m thickness and the threshold energy of muons is 1 GeV. Each muon detector consists of 50 rectangular proportional counters with an area of 5 m $\times$ 10 cm and 10 cm thickness, containing P10 gas (Ar, 90%; CH_4, 10%). The detailed characteristics of this type of proportional counter (PC) are described in Hayashida and Kifune (1980). The lateral distribution of electrons is determined with 156 surface detectors and the uncertainty of N_e determination is 20%. The lateral distribution of muons is determined between 50 m and 800 m from the core and the uncertainty of N_μ determination of each shower is 20%, provided the core position is well inside the array. The detailed analysis method is described in Nagano *et al* (1984a). The number of events included for this analysis is 995 457 recorded up to July 1992 for $N_e \geqslant 10^7$.

The 20 km^2 air shower array (hereafter denoted by A20, Teshima *et al* 1986) consists of 19 scintillation counters of area 2.2 m^2 each and four of area 1.0 m^2, which are distributed with about 1 km separation between detectors. A1 is situated at the eastern corner of A20. This array has operated since December 1984. Data are recorded whenever six or more neighbouring detectors out of 23 are triggered; at the same time, data from all detectors in A1 are recorded. From February 1990, this array has been part of the Akeno branch of the Akeno giant air shower array (AGASA). In this analysis, the Akeno branch data are added to those of A20 up to July 1992 and the number of events analysed is 43 482. Eight muon detectors of A1 are used for showers in A20.

AGASA, which has been operated since February 1990, consists of 111 scintillation

counters of area 2.2 m^2 each, deployed over a surface area of 100 km^2 (hereafter denoted by A100, Chiba *et al* 1992). Fourteen muon detectors have been available for AGASA since June 1991. The absorber is either concrete shielding or a combination of iron and lead, and the threshold energy is about 0.5 GeV. Proportional counters of the type found in A1 are used in AGASA; the length of each counter is 2 m or 5 m and the area of each detector is 2.8 m^2 or 10 m^2. The number of muon detectors was increased to 27 in April 1993, but the added detectors are not included in this analysis. The whole array is divided into four branches and data are recorded whenever five or more neighbouring detectors are triggered within each branch. The number of events analysed is 14 735, up to April 1993.

In all three experiments, primary energies, core positions and arrival directions of the showers are determined by the surface detectors and only showers with their core well inside each array are selected for further analysis. For A1 showers, N_e is used as an estimator of primary energy (E). The relation between N_e and E was derived in a previous experiment (Nagano *et al* 1984b) and is given by

$$E = 3.9 \times 10^{15} \left(\frac{N_e}{10^6} \right)^{0.9} \text{ eV}. \tag{1}$$

For showers measured by A20 and A100, the surface detector separations are about 1 km, and hence N_e cannot be determined in individual showers. Therefore, the charged-particle density at 600 m from the core, $S(600)$, which depends quite weakly on primary composition and the stage of shower development (Hillas *et al* 1971, Dai *et al* 1988), is used to estimate E:

$$E = 2.0 \times 10^{17} S(600)^{1.0} \text{ eV}. \tag{2}$$

In table 1, the durations and numbers of events analysed in each array are summarized.

Table 1. The durations and numbers of events analysed in each array.

Array	Duration of the experiment	Number of events	Energy range (eV)
A1	October 1981–July 1992	995 457	3×10^{16}–3×10^{18}
A20	December 1984–July 1992	43 482	3×10^{17}–3×10^{19}
A100	June 1991–April 1993	14 735	3×10^{17}–3×10^{19}

2.2. *Muon detector*

The numbers and areas of muon detectors used for the present analysis are listed in table 2 together with their threshold energy.

Table 2. The numbers and areas of muon detectors used for the present analysis.

Array	Area of one detector (m^2)	Number of detectors	Length of each PC (m)	Number of PC in each detector	Threshold muon energy (GeV)
A1	25.0	8	5.0	50	1.0
A20	25.0	8	5.0	50	1.0
A100	2.8	12	2.0	14	0.5
	10.0	2	5.0	20	0.5

The gain of each proportional counter used in these three experiments is adjusted to within ±3% by measuring the pulse height distribution of muons traversing the counter omnidirectionally. It has been confirmed experimentally that the peak position for omnidirectionally traversing muons is the same as that for vertically traversing muons. The average pressure of P10 gas in each counter is set to be a few per cent higher than the atmospheric pressure at the Akeno altitude (920 g cm^{-2}) at around 20° C. The output signal of each counter is shaped to an exponential form with a time constant of 20 μs and discriminated to give a square pulse at the level of a few tenths of a particle equivalent. The pulse width is proportional to the logarithm of the number of particles incident on a counter. The dynamic range of each counter is ~100 particles. The pulse width of each counter is recorded when air shower trigger conditions are satisfied in A1 and A20. In the case of A100, data are recorded whenever more than two counters separated by at least 10 cm are hit, or when the surface detector placed at the same position is hit. The gate widths for muon data capture are 8 μs for A1, 64 μs for A20 and 15.5 μs for A100. A short gate width can be used in A100, because the trigger time is assigned after adjustment for the delay time due to the cable length. This time is then examined in the stored data in cyclic memory. Accidental backgrounds were examined experimentally using random triggers for the three experiments separately and were determined to be 0.003 m^{-2} for A1, 0.022 m^{-2} for A20 and 0.003 or 0.006 m^{-2} for A100, depending on the materials used for the absorber (a combination of iron and lead, or concrete shielding).

The muon density (ρ_μ) in each detector is calculated by two methods, the so-called on–off density and analogue density methods. The on–off density is determined from the number of hit counters under the assumption that the number of particles incident on each counter follows a Poissonian distribution around the average value. In the case of n hit counters out of m available counters, ρ_μ is given by

$$\rho_\mu = -\frac{m \ln(1 - n/m)}{\text{Area}} \tag{3}$$

where Area is the total area of the detector. Provided showers are vertically incident and n is much smaller than m, this on–off density is a good measure of a real density. On the other hand, the analogue density is determined by the sum of energy losses in all counters divided by the average energy loss of a vertically traversing muon. Since the pulse height distribution is asymmetric with a long tail, reflecting a Landau fluctuation of energy losses in gas, the analogue density gives a larger value than the on–off density. This systematic factor depends on the distance from the core and is derived by comparing the analogue density with the on–off density. At distances more than a few 100 m from the core this value is 1.6. In this paper, the on–off density is used only for vertical showers and the analogue density is used for both vertical and inclined showers.

In the present analysis, the lateral distribution of muons was not determined for each shower. Muon densities, ρ_μ, are accumulated in a number of bins representing ranges of zenith angles (θ), N_e, local densities at 600 m from the core ($S(600)$) and core distances (R). After averaging ρ_μ in each bin, the average backgrounds are subtracted from the average densities.

3. Results

3.1. The lateral distribution of muons (LDM) for core distances ⩽ 800 m

First, the LDM for core distances (R) within 800 m from the core was studied. For this purpose, a data set obtained by A1 was used. In figure 2, the average ρ_μ in bins of width

$\Delta \log N_e = 0.25$ from $\log N_e = 7.0$ to $\log N_e = 9.0$ are plotted for vertical showers as a function of core distance. In each bin ρ_μ are normalized to the middle value of N_e. Those in bins of width $\Delta \sec\theta = 0.1$ are shown in figures 3(*a*) and (*b*) for two N_e ranges.

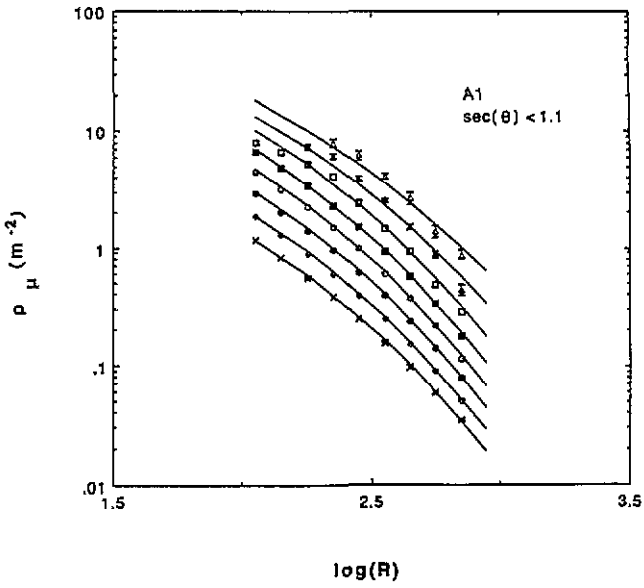

Figure 2. The average lateral distribution of muons obtained by A1 for vertical air showers ($\langle\sec\theta\rangle = 1.05$). Data are divided into eight bins of logarithmically equal size between 10^7 and 10^9 (cross, 10^7–$10^{7.25}$; diamond, $10^{7.25}$–$10^{7.5}$; full circle, $10^{7.5}$–$10^{7.75}$; open circle, $10^{7.75}$–$10^{8.0}$; full square, $10^{8.0}$–$10^{8.25}$; open square, $10^{8.25}$–$10^{8.5}$; full triangle, $10^{8.5}$–$10^{8.75}$; open triangle, $10^{8.75}$–$10^{9.0}$). The curves of best fit are shown by solid curves in each size bin.

To examine the N_e dependence or the zenith-angle dependence of the shape of the LDM, the formula given by Greisen (1960) was used

$$\rho_\mu(R) = N_\mu(C_\mu/R_0^2)\, r^{-\alpha}(1+r)^{-\beta} \tag{4}$$

where N_μ is the total number of muons, $r = R/R_0$ and R_0 is a characteristic distance. C_μ is a normalization factor, given by $C_\mu = \Gamma(\beta)/\{2\pi\Gamma(2-\alpha)\,\Gamma(\alpha+\beta-2)\}$. In the present analysis, the value of α was fixed to be 0.75, as determined by a previous analysis (Hayashida *et al* 1991).

β and R_0 were determined for vertical showers ($\sec\theta < 1.1$) by fitting ρ_μ to (4) using a least-squares method in each N_e bin. The best fitted values are $\beta = 2.52 \pm 0.04$ and $R_0 = 266 \pm 32$ m. The lines in figure 2 are drawn for the best fitted values of β and R_0 in each bin and no significant energy dependence has been found for either β or R_0. The zenith angle dependence of R_0 was determined using inclined showers with $\sec\theta < 1.8$ by keeping $\beta = 2.52$ constant for N_e between $10^{7.0}$ and $10^{9.0}$ and is expressed as

$$\log(R_0) = (0.58 \pm 0.04)(\sec\theta - 1) + (2.39 \pm 0.05) \tag{5}$$

where C_μ in (4) is 0.262. In general, increasing (or decreasing) β in (4) gives rise to a similar effect on the LDM to that produced by decreasing (or increasing) R_0. R_0 may be viewed as a parameter reflecting the muon production height. In figures 3(*a*) and (*b*) the curves are drawn using this equation. It is found that the LDM derived by Greisen in a much lower energy region is still a good expression for the showers of the present energy region

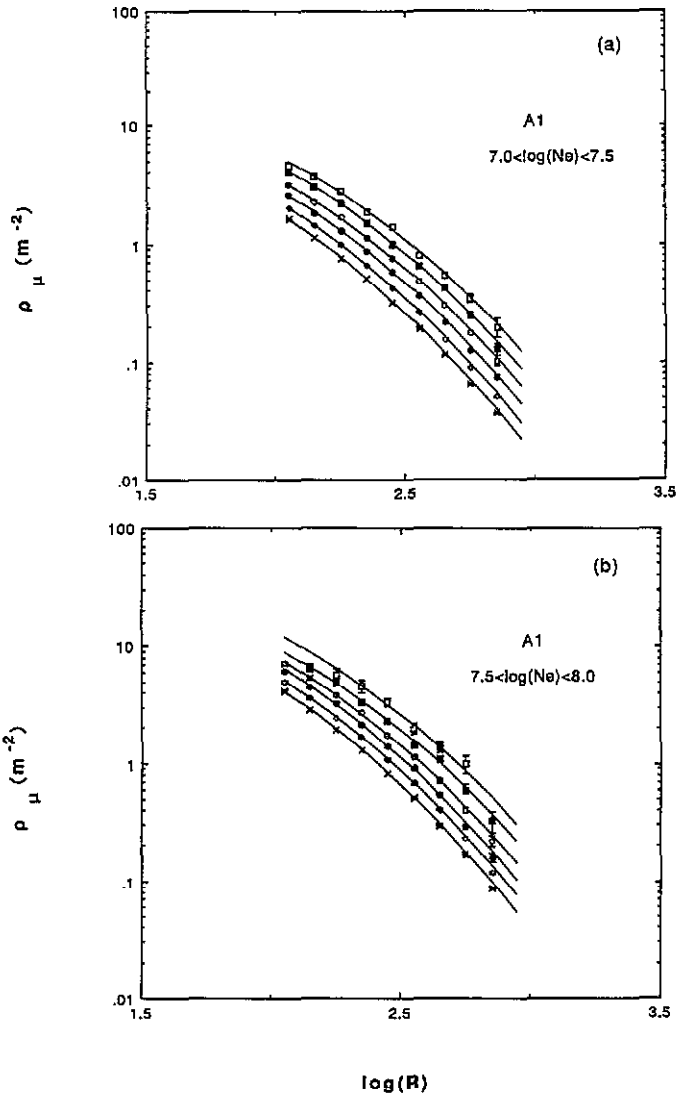

Figure 3. Zenith angle dependence of the lateral distribution of muons for $1.0 \leqslant \sec\theta < 1.6$ and $10^{7.0} \leqslant N_e < 10^{7.5}$ in (*a*) and $10^{7.5} \leqslant N_e < 10^{8.0}$ in (*b*). The curve of best fit is shown in each zenith angle bin (cross, $1.0 \leqslant \sec\theta < 1.1$; diamond, $1.1 \leqslant \sec\theta < 1.2$; full circle, $1.2 \leqslant \sec\theta < 1.3$; open circle, $1.3 \leqslant \sec\theta < 1.4$; full square, $1.4 \leqslant \sec\theta < 1.5$; open square, $1.5 \leqslant \sec\theta < 1.6$).

within 800 m from the core. ρ_μ cannot be determined in this experiment for $R > 800$ m owing to the restricted size of the 1 km^2 air shower array.

An example of a large shower observed by A1 is shown in figure 4.

3.2. LDM for core distances > 800 m

The LDM for core distances $250 \leqslant R < 2000$ m was investigated using data obtained by A20 for $10^{17.5} \leqslant E < 10^{19.5}$ eV for vertical showers ($\sec\theta < 1.2$). In the case of A20,

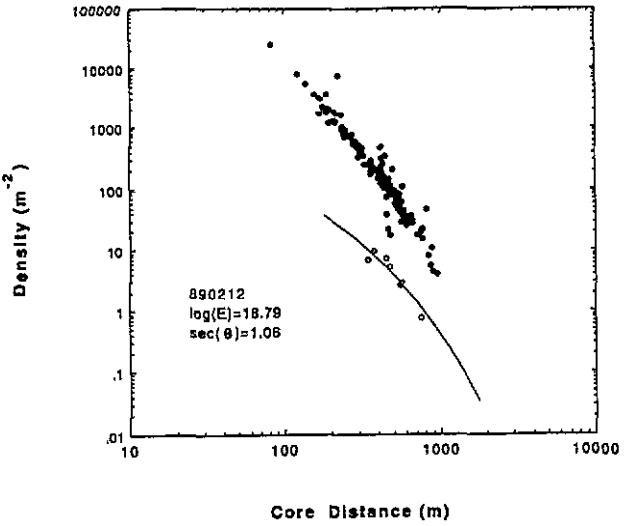

Figure 4. An example of the lateral distributions of charged particles (full circles) and muons (open circles) is shown for one of the biggest showers observed by A1. Shower parameters determined are $\log(E) = 18.79$ and $\sec\theta = 1.06$.

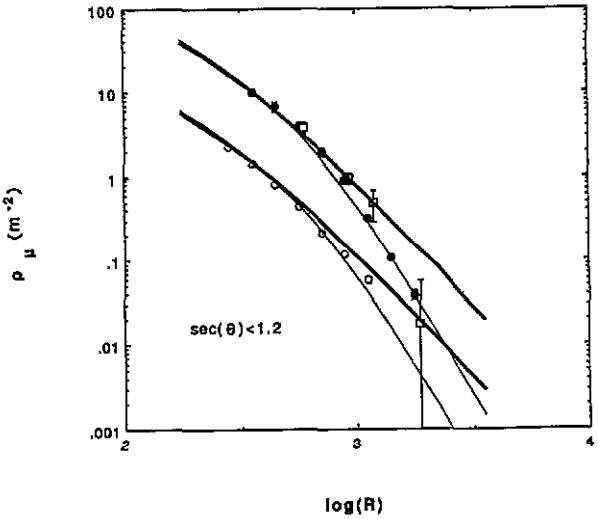

Figure 5. Lateral distribution of muons obtained by A20 and A100 for vertical showers ($\langle\sec\theta\rangle = 1.09$) in $10^{17.5} \leqslant E < 10^{18.0}$ eV (open circles) and $10^{18.5} \leqslant E < 10^{19.0}$ eV (full circles) normalized to $10^{17.75}$ eV and $10^{18.75}$ eV. The Greisen LDM represented by (4) and the modified LDM represented by (6) are shown by thick and thin solid curves, respectively. The experimental data are well represented by (6).

the average ρ_μ are determined with eight muon detectors of area 25 m^2, deployed inside A1 at positions 1.5–2.5 km distant from the centre of A20. Large area muon detectors are advantageous in investigating the LDM with R exceeding ~1000 m.

The average ρ_μ obtained from A20 are plotted with open and full circles as a function of core distance in figure 5 for two energy ranges. Here the ρ_μ are normalized to energies of $10^{17.75}$ eV and $10^{18.75}$ eV, respectively, and the average values are plotted. The thick

solid curves are those expected from (4) using β and R_0 obtained for $R \leqslant 800$ m; it can be seen that the data agree very well with these curves within 800 m from the core. However, they show significantly lower values than the extrapolated values of (4) for $R > 800$ m. The best fitted LDM up to 2000 m, shown by thin curves, is expressed by modifying (4) to give

$$\rho_\mu = N_\mu (C'_\mu / R_0^2)\, r^{-0.75}(1+r)^{-\beta}\left\{1 + (R/800\ \mathrm{m})^3\right\}^{-\delta} \tag{6}$$

where $\delta \sim 0.6$. C'_μ was calculated numerically to be 0.325 for $\beta = 2.52$. Independent measurements were also made for vertical showers using A100. In order to take into account the difference in muon threshold energies of A20 (> 1 GeV) and A100 (> 0.5 GeV), the densities from A100 were reduced by 1.4, a value obtained from a previous experiment (Matsubara *et al* 1985). Muon densities from A100, adjusted to a threshold of 1 GeV, are plotted in figure 5 with squares for $10^{18.5}$–10^{19} eV. They are consistent with ρ_μ from A20 within experimental errors.

The number of inclined showers ($\sec\theta \geqslant 1.2$) is not large enough to determine the zenith angle dependence of the LDM up to 2000 m. The zenith angle dependence is discussed in terms of $\rho_\mu(600)$ in section 4.2.

3.3. The relation between N_μ and N_e

The average N_μ is determined for data obtained by A1 by integrating (4) for a number of N_e bins using β and R_0 obtained above. The average N_μ is plotted in figure 6(*a*) as a function of N_e for vertical showers ($\sec\theta < 1.1$). N_μ is also plotted in figure 6(*b*) as a function of $\sec\theta$ for three different N_e bins. N_μ is expressed as a function of N_e and $\sec\theta$ by

$$N_\mu = (2.6 \pm 1.4) \times 10^{5.0+a}(N_e/10^7)^b \tag{7}$$

for $10^{7.0} \leqslant N_e < 10^{8.5}$ and $\sec\theta \leqslant 1.6$, where $a = (1.07 \pm 0.13)(\sec\theta - 1)$ and $b = (0.77 \pm 0.02) - (0.17 \pm 0.02)(\sec\theta - 1)$.

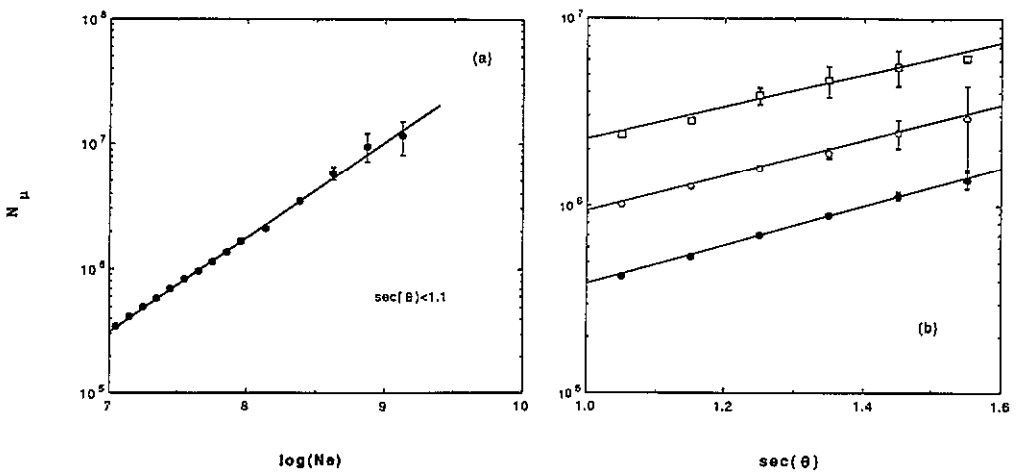

Figure 6. The average N_μ is plotted as a function of N_e for vertical showers ($\langle\sec\theta\rangle = 1.05$) in (*a*) and as a function of $\sec\theta$ for inclined showers ($1.0 \leqslant \sec\theta < 1.6$) in (*b*). Data for inclined showers are divided into three size regions (full circle, 10^7–$10^{7.5}$; open circle, $10^{7.5}$–10^8; open square, 10^8–$10^{8.5}$). The lines drawn are the average relations between N_μ and N_e obtained by A1 and expressed by (7).

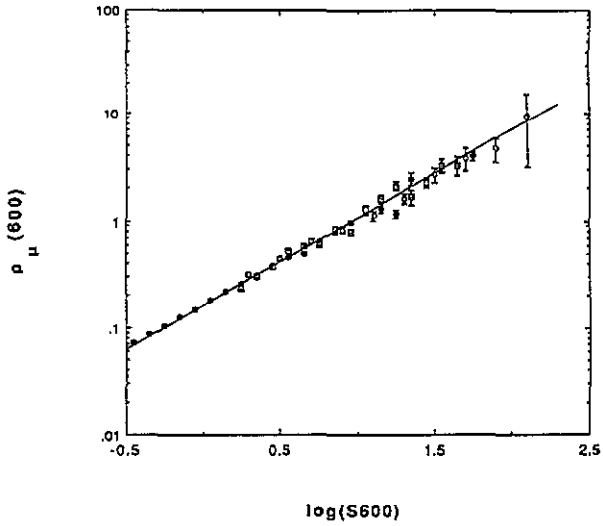

Figure 7. The average $\rho_\mu(600)$ is plotted as a function of $S(600)$ for A1 (closed circles), A20 (dotted squares), and A100 (open circles) for vertical showers ($< \sec\theta >= 1.09$). Data from A100 are normalized to those from A20. The solid lines represent (8).

3.4. The relation between $\rho_\mu(600)$ and $S(600)$

In the case of A20, the 1 km separation of muon detectors makes it difficult to integrate (6). It is also difficult to determine N_μ with A100 (for $E \leqslant 10^{19.0}$ eV), since the detectors have much smaller areas and are separated by larger distances than in A1. If the LDM does not change in the energy region concerned, the muon density at 600 m from the core, $\rho_\mu(600)$, is expected to be an estimator of N_μ, in the same way as $S(600)$ is an estimator of E_p. $\rho_\mu(600)$ is derived from an observed density at 500–800 m from the core, which is normalized to that at 600 m using (6).

Figure 7 shows the relation between $\rho_\mu(600)$ and $S(600)$ obtained by both A20 and A100 for vertical showers ($\sec\theta < 1.2$) for $10^{17.5} \leqslant E < 10^{19.5}$ eV. Densities from A100 are normalized to those from A20 ($\rho_\mu(600) = 2.66$) and the slopes of the relations between $\rho_\mu(600)$ and $S(600)$ from A100 and A20 agree with each other. The average $\rho_\mu(600)$ at $\langle\sec\theta\rangle = 1.09$ is expressed as a function of $S(600)$ by

$$\rho_\mu(600) = (0.16 \pm 0.01) \times S(600)^{0.82\pm0.03}. \tag{8}$$

The $\rho_\mu(600)$ data obtained from A1 for the same zenith angle bin are also shown in figure 7 and are consistent with the other plots. The average $\rho_\mu(600)/S(600)$ at $\langle\sec\theta\rangle = 1.09$ for A20 and A100 are expressed as

$$\rho_\mu(600)/S(600) = (0.17 \pm 0.01) \times S(600)^{-0.20\pm0.02}. \tag{9}$$

4. Discussion

4.1. Comparison of LDM with other experiments

In figure 8, we plot $\rho_\mu \times R^2$ for vertical showers ($\sec\theta < 1.2$) obtained by A20 normalized to $10^{18.75}$ eV to display the distribution more clearly. The vertical atmospheric depth of Akeno is 920 g cm^{-2}, which is shallower than those of Sydney (980 g cm^{-2}) and Yakutsk

(1020 g cm^{-2}). In the figure, results of these two experiments at the atmospheric depth of 1020 g cm^{-2} are compared, where the threshold energy of muons in the Sydney and Yakutsk experiments is $0.75 \sec\theta$ GeV and $1.0 \sec\theta$ GeV, respectively. The corresponding $\sec\theta$ at the atmospheric depth of 1020 g cm^{-2} are 1.11 for Akeno, 1.04 for Sydney and 1.0 for Yakutsk. The average zenith angle of the Akeno results is $\sec\theta = 1.09$ which does not differ greatly from $\sec\theta = 1.11$.

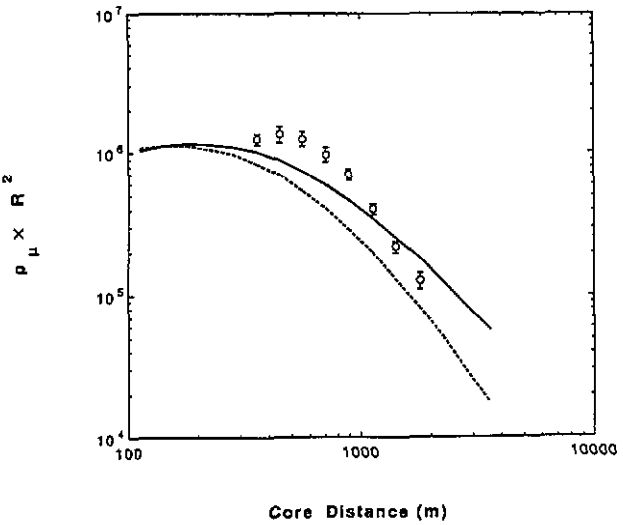

Figure 8. LDM obtained by A20 for vertical showers ($\langle\sec\theta\rangle = 1.09$) is compared with those obtained by the Yakutsk group and the Sydney group. Data from A20 are plotted with open circles normalized to $10^{18.75}$ eV and data from the Yakutsk group are represented by a dotted curve. The solid curve is the average LDM of the Sydney group.

The LDM of the Sydney group is expressed by Greisen's formula in which β in (4) is a function of $\sec\theta$ with a constant R_0 (Winn *et al* 1986) and is shown in the same figure by a solid curve. The data from A20 show a steeper lateral distribution than the Sydney LDM. In the case of the Sydney experiment, there may be a triggering bias favouring showers with flatter muon lateral distributions. Furthermore, since only muon detectors are used in that experiment, the determination of the core position and the LDM are correlated. On the other hand, the LDM from A20 is determined independently of the array triggering and core position determination.

The LDM of the Yakutsk group recently reported by Glushkov *et al* (1994) is a modified version of Greisen's formula similar to (6) and is shown in figure 8 by a dotted curve. The modification factor is $(1 + R/2000)^{-1}$ instead of $(1 + (R/800)^3)^{-0.6}$ and β is a function of $\sec\theta$ instead of R_0. The shape of the LDM is consistent with the results of A20 over the core distances concerned. However, the Yakutsk LDM extrapolated inside 300 m from the core is much steeper than the Akeno result. The absolute value of the LDM obtained by the Sydney group is smaller than that of A20 by a factor of 1.5, while that of the Yakutsk group is smaller by a factor of 1.8, if compared at $R = 600$ m from the core.

On the other hand, the N_μ at $10^{18.75}$ eV obtained by the Akeno, Yakutsk and Sydney groups using their LDMs are 2.5×10^7, 2.2×10^7 and 3.1×10^7, respectively. These values do not differ greatly in this energy region, even though the shapes of the LDMs are different and the primary energy assignment method is different in each experiment. The conversion relation between N_μ and E is discussed in section 4.3.

4.2. Comparison of $\rho_\mu(600)/S(600)$ with the Yakutsk experiment

To examine changes in shower characteristics in the energy region above 5×10^{18} eV claimed by Glushkov *et al*, the average ratios of $\rho_\mu(600)$ to $S(600)$ obtained by A1, A20 and A100 are plotted as a function of $S(600)$ in figure 9 for five different zenith angle bins. $S(600)$ values corresponding to 5×10^{18} eV at each zenith angle bin are shown by arrows in the figures. In order to convert $S(600)$ to a primary energy an attenuation of $S(600)$ described in Yoshida *et al* (1994) is taken into account. No significant change in the slopes of the ratios is observed even above 5×10^{18} eV. The ratios are fitted to the following equation and are shown by solid lines

$$\log\rho_\mu(600)/S(600) = A\log S(600) + B. \tag{10}$$

Values of A and B derived by a least-squares method are listed in table 3.

The ratio from the Yakutsk experiment for $1.8 \leqslant \sec\theta < 2.0$ is estimated from figure 10 of Glushkov *et al* (1994) and is shown by a dotted line in figure 9(*e*). Our present results for $E \geqslant 5\times10^{18}$ eV are consistent with extrapolations from lower energy regions for $\sec\theta < 2.0$. The behaviour seen in the Yakutsk results has not been observed. Confirmation of the present result, however, requires further accumulation of data.

Table 3. Values of A and B defined in (10), which show the relation between $\rho_\mu(600)/S(600)$ and $S(600)$, are listed as a function of $\sec\theta$.

$\sec\theta$	A	B
1.0–1.2	−0.17 ± 0.01	−0.76 ± 0.01
1.2–1.4	−0.16 ± 0.01	−0.58 ± 0.01
1.4–1.6	−0.17 ± 0.04	−0.40 ± 0.02
1.6–1.8	−0.22 ± 0.10	−0.30 ± 0.03
1.8–2.0	−0.30 ± 0.22	−0.21 ± 0.06

4.3. Conversion between N_μ and E

To determine the energy spectrum of primary particles from the N_μ spectrum (as done in the Sydney experiment), one needs the conversion relation from N_μ to E or from $\rho_\mu(600)$ to E. In section 3.3, the conversion relation from N_e to N_μ was obtained by A1 as (7), while N_e is converted into E using (1). These two equations are combined into

$$\log N_\mu = (0.84\pm0.02)\log E - (8.38\pm0.35) \tag{11}$$

at $\sec\theta = 1.0$. The conversion relation from N_μ to E is expressed by

$$E = 2.16\times10^{18}(N_\mu/10^7)^{1.19}\ \text{eV}. \tag{12}$$

This relation is in agreement with our previous result within experimental errors (Nagano *et al* 1984b).

The conversion relation from N_μ to E derived by the Yakutsk group is expressed as

$$E = 2.48\times10^{18}(N_\mu/10^7)^{1.05}\ \text{eV}.$$

After taking into account the difference in the depths of the Yakutsk and Akeno experiments (100 g cm^{-2}), we find good agreement in the energy conversion relations, even though the LDMs are inconsistent. Good agreement is not found with the relation used by the SUGAR experiment, which is derived from simulations (model E) by Hillas *et al* (1971)

$$E = 1.64\times10^{18}(N_\mu/10^7)^{1.075}\ \text{eV}.$$

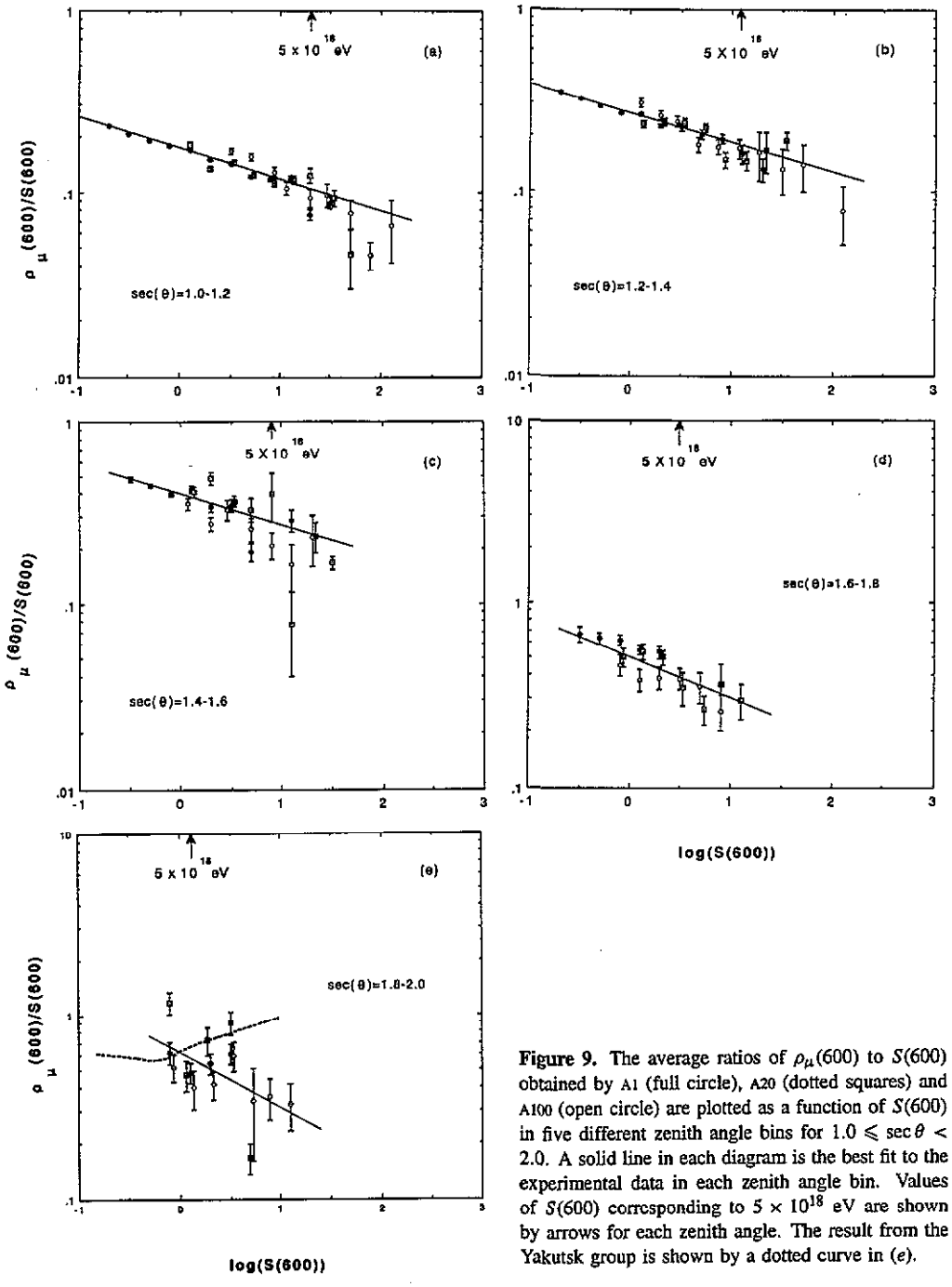

Figure 9. The average ratios of $\rho_\mu(600)$ to $S(600)$ obtained by A1 (full circle), A20 (dotted squares) and A100 (open circle) are plotted as a function of $S(600)$ in five different zenith angle bins for $1.0 \leqslant \sec\theta < 2.0$. A solid line in each diagram is the best fit to the experimental data in each zenith angle bin. Values of $S(600)$ corresponding to 5×10^{18} eV are shown by arrows for each zenith angle. The result from the Yakutsk group is shown by a dotted curve in (*e*).

The relation between $\rho_\mu(600)$ and $S(600)$ obtained by A20 and A100 can be converted into one between E and ρ_μ by using (2) and (8). The relation at $\sec\theta = 1.0$ is

$$E = 2.22 \times 10^{18} \rho_\mu(600)^{1.22} \text{ eV}. \tag{13}$$

Assuming β, R_0 and δ in (6) are independent of primary energy, this relation can be converted to a relation between N_μ and E at $\sec\theta = 1.0$

$$\log N_\mu = (0.82 \pm 0.03) \log E - (8.06 \pm 0.04). \tag{14}$$

Relations (11) and (14) are smoothly connected with each other within experimental errors for the range $10^{16.5} \leqslant E < 10^{19.5}$ eV, although the overlapping region is only $10^{17.5} \leqslant E < 10^{18.5}$ eV.

4.4. Comparison of the present LDM with the simulated LDM

The LDM beyond 800 m from the core cannot be expressed by Greisen's formula (4). It becomes significantly steeper than the extrapolated values of (4) and the muon density at $R = 2000$ m is about 20% of the extrapolated value. Simulated values at distances far from the core for EAS of energy 10^{19} eV are available from simulations performed by Cronin (1994a) at the atmospheric depth of 1000 g cm^{-2} using a program prepared by Hillas (MOCCA).

The lateral distributions of both charged particles and muons are compared simultaneously in the form of density $\times R^2$. The lateral distribution of charged particles obtained by AGASA has been reported in Yoshida *et al* (1994). $S(600)$ at 1000 g cm^{-2} is evaluated as 36.5 m^{-2} at 10^{19} eV with the difference in the Moliere length taken into account. $\rho_\mu(600)$ at 1000 g cm^{-2} is derived from (8) using 42.5 as $S(600)$, which is obtained at $\sec\theta = 1.09$ at Akeno level for 10^{19} eV. The Akeno results are shown in figure 10 by a thin solid curve for charged particles and a thick solid curve for muons. The average energy deposit per m^2 in a 50 mm thick scintillator calculated by the MOCCA program is compared with the lateral distribution of charged particles obtained by Akeno and denoted

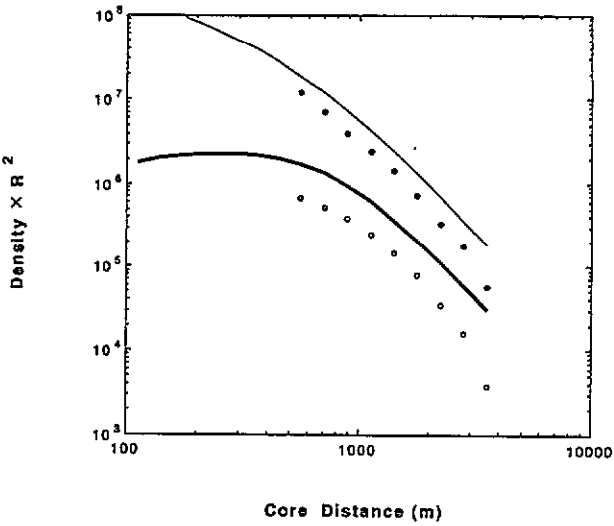

Figure 10. Lateral distributions of muons and charged particles obtained by the Akeno experiment are compared at the atmospheric depth of 1000 g cm^{-2} with the simulation results of protons at 10^{19} eV by Cronin using the MOCCA program provided by Hillas. A full circle shows the average energy deposit per m^2 in a 50 mm thick scintillator and an open circle corresponds to the muon density for > 1 GeV. Lateral distributions of charged particles and muons obtained by this experiment are shown by a thin and a thick solid curve, respectively.

by a full circle. The simulated muon density (> 1 GeV) is also shown in the same figure as an open circle.

The charged-particle density obtained by the Akeno result exceeds the prediction of MOCCA by a factor of 1.4 at 600 m from the core and 1.9 at 2000 m. The Akeno result for muon densities also exceeds that predicted by MOCCA by factors of 2.0 and 2.3 at 600 m and 2000 m from the core, respectively. If the density of charged particles is normalized at 600 m from the core, the muon density obtained by the Akeno experiment is a factor of 1.5 greater than the prediction of MOCCA at 600 m from the core. Except for these differences in absolute values, the lateral distributions of both charged particles and muons obtained by Akeno are quite consistent in shape with the prediction by MOCCA simulations.

Table 4 lists typical densities (per m^2) at $\sec\theta = 1.0$, estimated from the present experiment.

Table 4. Typical densities (per m^2) at $\sec\theta = 1.0$ estimated from the present experiment.

Primary energy	$S(600)$	$S(1000)$	$S(1500)$	$\rho_\mu(600)$	$\rho_\mu(1000)$	$\rho_\mu(1500)$
1×10^{19} eV	50	6.6	1.1	3.4	0.57	0.10
3×10^{19} eV	150	20	3.4	8.4	1.4	0.25
1×10^{20} eV	500	66	11	22	3.7	0.66

4.5. Composition of cosmic rays

Assuming the validity of the superposition model for the development of showers initiated by nuclei, the elongation rate ($\delta X_{\max}/\delta \ln E$) can be related to a mass A by

$$\frac{\delta X_{\max}}{\delta \ln E} = a\left(1 - \frac{\delta \ln A}{\delta \ln E}\right)$$

or

$$X_{\max} = a \ln\left(\frac{E}{A}\right) + b.$$

Similarly,

$$\frac{\delta \ln N_\mu}{\delta \ln E} = \alpha + (1 - \alpha)\frac{\delta \ln A}{\delta \ln E} \tag{15}$$

where α is related by

$$N_\mu = k(A)E^\alpha.$$

Therefore, if the change in elongation rate around 3×10^{17} eV observed with the Fly's Eye data is due to a change in composition ($\delta \ln A/\delta \ln E \sim -0.58$), a change of slope in the relation between N_μ and E may be expected around 3×10^{17} eV. In the following, any changes in ($\delta \ln N_\mu/\delta \ln E$) are investigated by replacing N_μ by $\rho_\mu(600)$ and E by $S(600)$.

Relations between the densities of muons (ρ_μ) and those of all charged particles (S) at various core distances were exhibited by Dawson (1993) for simulated proton and iron primaries. There is a factor of 1.7 difference in ρ_μ for iron and proton primaries at constant S, suggesting the view that there must be an observable change in the slope of the relation between N_μ and $S(600)$ if there is a change in composition from a predominantly heavy to a light composition. If there were a systematic change in the chemical composition of primary cosmic rays between $10^{17.5}$ eV and $10^{18.5}$ eV, a possible change in the relation

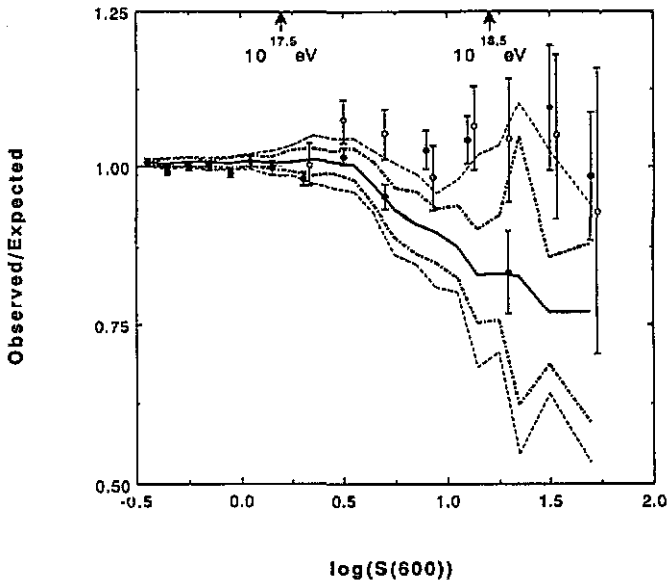

Figure 11. $\rho_\mu(600)$ divided by the expected values are plotted as a function of $S(600)$ between $10^{16.5}$ eV and 10^{19} eV. The expected densities are extrapolations from the average relation determined below $10^{17.5}$ eV. Data from A1 (full circles), A20 (open circles) are included. Data from A100 are combined with those from A20 after normalizing the threshold energy of muons. Values of $S(600)$ corresponding to $10^{17.5}$ eV and $10^{18.5}$ eV are shown by arrows. An expectation from the composition model proposed by the Fly's Eye group is shown by dotted curves *(90% CL), chain curves (68% CL) and a solid curve (the average), respectively.*

between N_μ and N_e (equation (7)), or in the relation between $\rho_\mu(600)$ and $S(600)$ (equation (8)), might be expected.

The relation between $\rho_\mu(600)$ and $S(600)$ was examined for vertical showers ($\sec\theta < 1.2$) and compared with that extrapolated from the relation determined in the energy region below $10^{17.5}$ eV. Expected values of $\rho_\mu(600)$ were derived from the results of A1 for $-0.5 \leqslant \log S(600) < 0.2$. Contributions from accidental backgrounds exceed 5% of densities measured for $\log S(600) < -0.5$, therefore data in this energy region were not used. $\rho_\mu(600)$ for A1, A20 and A100 normalized to those of A20, were divided by the expected muon density given by (8) with $b = 0.82$ and are plotted in figure 11 over the whole $S(600)$ range. Data from A100 are combined with those from A20. The two vertical arrows in the figure correspond to $10^{17.5}$ eV and $10^{18.5}$ eV, respectively. No systematic change in the ratio of the observed and expected $\rho_\mu(600)$ can be seen for $E \geqslant 10^{17.5}$ eV.

Table 5. $\rho_\mu(600)$ measured by each detector in A1 is summed and compared with the expected value. 'Deficit' is defined in the text. The deficit ranges were simulated assuming the two-component composition model proposed by the Fly's Eye group and are listed at 68% confidence level.

Experiment	$\sum_{\text{total events}} \rho_\mu(600)$	Deficit	Simulation
A1 ($> 10^{17.5}$ eV)	3.95×10^4	$(-1.5 - -0.8) \pm 0.5\%$	$(-4.8 - -1.2)\%$
($> 10^{18.5}$ eV)	2.45×10^3	$(-2.8 - 0.4) \pm 2.0\%$	$(-25.8 - -15.0)\%$

In order to examine a possible change quantitatively, $\rho_\mu(600)$ measured by each detector in A1 is summed for all events with $E \geqslant 10^{18.5}$ eV and is equal to 2449. The value expected from the extrapolation of the relation between $\rho_\mu(600)$ and $S(600)$ determined in the energy range below $10^{17.5}$ eV is estimated to be 2440–2517. The reduced proportion of observed muon particles compared with the expected number (hereafter called the 'deficit') is $(-2.8\text{–}0.4) \pm 2.0\%$. The number of muons above $10^{17.5}$ eV is 3949×10^4, whereas $(3983\text{–}4007) \times 10^4$ are expected from the linear extrapolation of the lower energy results. The observed number shows a deficit of $(-1.5 - -0.8) \pm 0.5\%$. These comparisons of integrated $\rho_\mu(600)$ with the expected values are presented in table 5.

Assuming the two-component composition model proposed by the Fly's Eye group, the expected relation between $\rho_\mu(600)$ and $S(600)$ in the present experiment was estimated by a Monte Carlo simulation making the following assumptions:

(i) $S(600)_{Fe}/S(600)_p = 1.04$. From Cronin (1994b) and Dawson (1993).
(ii) Fluctuation of $S(600)_{Fe} = 15\%$ and $S(600)_p = 15\%$. From figure 2(*a*) of Dawson (1993).
(iii) $\rho_\mu(600)_{Fe}/\rho_\mu(600)_p = 1.7$. From Cronin (1994b) and Dawson (1994).
(iv) Fluctuation of $\rho_\mu(600)_{Fe} = 10\%$ and $\rho_\mu(600)_p = 15\%$. From figure 2(*a*) of Dawson (1993).
(v) $S(600)_p$ and $S(600)_{Fe}$ are proportional to $E^{1.0}$. From figure 3 of Dawson (1993).
(vi) $\rho_\mu(600)_p$ and $\rho_\mu(600)_{Fe}$ are proportional to E^α, $\alpha = 0.84$. From Dawson (1994).
(vii) Energy dependence of the composition of primary cosmic rays. A two-composition model proposed from the Fly's Eye experiment (Bird *et al* 1994).
(viii) Absolute value of $\rho_\mu(600)$. Normalized to the experiment at $10^{17.5}$ eV.
(ix) Primary energy spectrum. Akeno spectrum from Yoshida *et al* (1995).
(x) The error in determining $S(600)(\sigma_{S(600)})$. 20% (section 2.1). $S(600)$ is derived from N_e in the case of A1.
(xi) The determination of $\rho_\mu(600)$. Determined from experimental points from 25 m^2 detectors, between 500 m and 800 m from the core, by interpolating with LDM expressed by (6).
(xii) The error in determining $\rho_\mu(R)$. Poisson distribution over area 25 m^2. On–off density is used for vertical showers.

In this simulation, events were accumulated until the total number of events amounted to the same number as seen by the experiment. The relation between $\rho_\mu(600)$ and $S(600)$ was determined below $10^{17.5}$ eV in each simulation and the $\rho_\mu(600)$ values from more energetic showers were compared with those expected from the extrapolation of this relation. In total 50 data sets were simulated. A 68% confidence level (CL) and a 90% CL in each $S(600)$ are determined and shown in figure 11 by chain and dotted curves, respectively. The deficit ranges estimated by the simulation are listed in table 5 at 68% CL. The deficit in the ratio of the observed and expected values ranges from −4.8% to −1.2% for $E \geqslant 10^{17.5}$ eV at 68% CL over the 50 simulations. The experimental result is consistent with this range. However, the deficit extends from −25.8% to −15.0% for $E \geqslant 10^{18.5}$ eV at 68% CL. The range corresponding to a 90% CL is −31.2 to −11.1%, while the experimental deficit is significantly smaller than this value. Therefore, the simple two-component model proposed by the Fly's Eye group cannot be supported by our experiment under the assumptions of the present simulation.

The relation between $\rho_\mu(600)$ and $S(600)$ obtained from the present experiment is expressed by (8) and the exponent (0.82 ± 0.03) is in good agreement with the simulated value, 0.84. If we use assumption (vi) of the simulation above and relation (15), the

expected ratio for a changing composition given by $\delta \ln A/\delta \ln E = -0.58$ almost coincides with the average line of figure 11 and is consistent with the simulation. In order to satisfy our experiments, $(\delta \ln A/\delta \ln E)$ may be greater than -0.3 which is near to an upper chain curve in figure 11; that is, the rate of change of composition may be less than half of the Fly's Eye group's interpretation. We need further accumulation of data and more detailed simulations in order to determine the composition of primary cosmic rays by measuring relations between $\rho_\mu(600)$ and $S(600)$.

5. Summary

The LDM was first determined by experiment A1 for core distances $\leqslant 800$ m and $10^{16.5}$ eV $\leqslant E < 10^{18.5}$ eV for both vertical and inclined showers. The parameters which determine the LDM are consistent with those reported previously and are expressed by equation (4) (Hayashida *et al* 1991). However, the LDM for core distances beyond 800 m becomes significantly steeper compared with the extrapolation of (4) for showers between $10^{17.5}$ eV and $10^{19.5}$ eV. The shape of the LDM is in agreement, within statistical errors, with both the Yakutsk result and the simulation results from the MOCCA program for core distances beyond 300 m. However, the absolute value exceeds both of these by a factor of ~2.0–2.5.

The energy dependence of the ratio of $\rho_\mu(600)$ to $S(600)$ is examined for five zenith angle ranges and no significant deviation from the expected dependence is observed up to 10^{19} eV for $\sec\theta < 2.0$.

The relation between N_μ and N_e is expressed in (7) for $10^{16.5} \leqslant E < 10^{18.0}$ eV, where N_μ is found to be proportional to $N_e^{0.77}$ for vertical showers. At higher energies it is shown that $\rho_\mu(600)$ is proportional to $S(600)^{0.82}$ for $10^{17.5}$–$10^{19.0}$ eV. The systematic change in the chemical composition of cosmic rays above $10^{17.5}$ eV claimed by the Fly's Eye group under the assumption of a simple two-component model was investigated using the relation between $\rho_\mu(600)$ and $S(600)$. This change in the composition cannot be confirmed within the present experimental uncertainties. The present experiment suggests a much smaller rate of change of composition between $10^{17.5}$ eV and $10^{18.5}$ eV.

Acknowledgments

The authors are indebted to Akeno-mura, Sudama-cho, Nagasaka-cho, Takane-cho and Ohoizumi-mura for their kind cooperation. They are also indebted to the other members of the Akeno group for their maintenance of the array and analysis of the A1 data.

The data analysis was partly carried out by FACOM M780 at the Computer Room, Institute for Nuclear Study, University of Tokyo. The authors thank Professor J Cronin and Dr B Dawson for valuable discussions and for providing us with their simulation results. We are also indebted to Dr B Dawson for helping with the preparation of the manuscript.

References

Bird D J *et al* 1993 *Proc. 23rd Int. Cosmic Ray Conf. (Calgary)* vol 2 p 38
Bird D J *et al* 1994 *Astrophys. J.* **424** 491
Chiba N *et al* 1992 *Nucl. Instrum. Methods* A **311** 338
Cronin J W 1992 *Preprint* EFI 92–8 University of Chicago
——1994a Private communication
——1994b *Preprint* Contribution to Snowmass report on cosmic rays (August, 1994)
Dai H Y, Kasahara K, Matsubara Y, Nagano M and Teshima M 1988 *J. Phys. G: Nucl. Phys.* **13** 793

Dawson B R 1993 *Proc. Tokyo Workshop on Techniques for the Study of Extremely High Energy Cosmic Rays* ed M Nagano (Tokyo: Institute for Cosmic Ray Research, University of Tokyo) p 125
——1994 Private communication
Glushkov A V, Makarov I T, Nikiforova E S, Pravdin M I and Sleptsov I Ye 1994 *J. Nucl. Phys. Preprint*
Greisen K 1960 *Ann. Rev. Nucl. Sci.* **10** 63
Hara T *et al* 1979 *Proc. 16th Int. Cosmic Ray Conf. (Kyoto)* vol 8 p 135
Hayashida N 1994 *Phys. Rev. Lett.* **73** 3491
Hayashida N and Kifune T 1980 *Nucl. Instrum. Methods* **173** 431
Hayashida N *et al* 1991 *Proc. 22nd Int. Cosmic Ray Conf. (Dublin)* vol 4 p 331
Hillas A M 1992 *Nucl. Phys.* B *(Proc. Suppl.)* **28** 67
Hillas A M, Marsden D J, Hollows J D and Hunter H W 1971 *Proc. 12th Int. Cosmic Ray Conf. (Hobart)* vol 3 p 1001
Matsubara Y, Hara T, Hayashida N, Kamata K, Nagano M, Ohoka H, Tanahashi G and Teshima M 1985 *Proc. 19th Int. Cosmic Ray Conf. (La Jolla)* vol 7 p 119
Nagano M, Hara T, Hatano Y, Hayashida N, Kamata K, Kawaguchi S, Kifune T and Tanahashi G 1984a *J. Phys. Soc. Japan* **53** 1667
Nagano M, Hara T, Hatano Y, Hayashida N, Kamata K, Kawaguchi S, Kifune T and Mizumoto Y 1984b *J. Phys. G: Nucl. Phys.* **10** 1295
Nagano M, Teshima M, Matsubara Y, Dai H Y, Hara T, Hayashida N, Honda M, Ohoka H and Yoshida S 1992 *J. Phys. G: Nucl. Part. Phys.* **18** 423
Teshima M *et al* 1986 *Nucl. Instrum. Methods* A *247* 399
Winn M M, Ulrichs J, Peak L S, McCusker C B A and Horton L 1986 *Catalogue of Highest Energy Cosmic Rays* ed A Inoue (Tokyo: World Data Center C2 for Cosmic Rays, Institute of Physics and Chemical Research)
Yoshida S *et al* 1994 *J. Phys. G: Nucl. Part. Phys.* **20** 651
Yoshida S1995 *Astroparticle Phys.* **3** 105